RESEARCH ARTICLE

PET Imaging of the P2X7 Ion Channel with a Novel Tracer [18F]JNJ-64413739 in a Rat Model of Neuroinflammation

Tamara Berdyyeva, Chunfang Xia, Natalie Taylor, Yingbo He, Gang Chen, Chaofeng Huang, Wei Zhang, Hartmuth Kolb, Michael Letavic, Anindya Bhattacharya, Anna Katrin Szardenings

Janssen Research & Development LLC, 3210 Merryfield Row, San Diego, CA, 92121, USA

Abstract

Purpose: The P2X7 receptor, an adenosine triphosphate (ATP)-gated purinoreceptor, has emerged as one of the key players in neuroinflammatory processes. Therefore, developing a positron emission tomography (PET) tracer for imaging of P2X7 receptors *in vivo* presents a promising approach to diagnose, monitor, and study neuroinflammation in a variety of brain disorders. To fulfill the goal of developing a P2X7 PET ligand as a biomarker of neuroinflammation, [18F]JNJ-64413739 has been recently disclosed.

Procedures: We evaluated [18F]JNJ-64413739 in a rat model of neuroinflammation induced by an intracerebral injection of lipopolysaccharide (LPS). *In vivo* brain uptake was determined by PET imaging. Upregulation of neuroinflammatory biomarkers was determined by quantitative polymerase chain reaction (qPCR). Distribution of the tracer in the brain was determined by *ex vivo* autoradiography (ARG). The specificity of [18F]JNJ-64413739 was confirmed by performing blocking experiments with the P2X7 antagonist JNJ-54175446.

Results: Brain regions of rats injected with LPS had a significantly increased uptake (34 % ± 3 % s.e.m., $p = 0.036$, t test, standardized uptake value measured over the entire scanning period) of [18F]JNJ-64413739 relative to the corresponding brain regions of control animals injected with phosphate-buffered saline (PBS). The uptake in the contralateral regions and cerebellum was not significantly different between the groups of animals. The increase in uptake of [18F]JNJ-64413739 at the LPS-injected site observed by PET imaging was concordant with *ex vivo* ARG, upregulation of neuroinflammatory biomarkers, and elevated P2X7 expression levels.

Conclusions: While further work is needed to study [18F]JNJ-64413739 in other types of neuroinflammation, the current results favorably characterize [18F]JNJ-64413739 as a potential PET tracer of central neuroinflammation.

Key words: P2X7 receptor, Neuroinflammation, Positron emission tomography (PET), PET imaging, [18F]JNJ-64413739, Lipopolysaccharide, LPS, Rats

---

Correspondence to: Tamara Berdyyeva; e-mail: tberdyy6@its.jnj.com

Introduction

Neuroinflammation is thought to play a role in many neuropsychiatric and neurological conditions [1–4]; however, its exact contribution remains poorly understood [5–7]. This is partially due to limited diagnostic tools to measure inflammation in the central nervous system (CNS) [8]. Positron emission tomography

(PET) enables non-invasive visualization and quantification of molecular targets within CNS [9]. Development of specific PET ligands for key neuroinflammatory targets would allow assessing the role of these targets in different brain diseases and aid selection of appropriate anti-neuroinflammatory treatment [10].

Recently, several targets have been investigated for PET imaging of neuroinflammation [11–18]. Specifically, multiple PET tracers binding the 18-kDa translocator protein (TSPO) have been evaluated in psychiatric [1] and neurodegenerative disorders [2, 19, 20]. There was limited success [21–24], but also failures [25–30]. Some failures were due to existing genetic polymorphisms affecting TSPO binding in humans [31–33]. While this limitation can be corrected [34–37], the non-specific role of TSPO in neuroinflammation are more difficult to address [9, 38, 39], as TSPO is involved in many cellular functions not specific to central inflammation [40–44].

In contrast, P2X7 receptor activation lies upstream of a cascade of events leading to microglial activation [45–47]. P2X7 receptor activation is causally linked to the production of proinflammatory cytokines within the brain [48–50]. Therefore, P2X7 receptor PET tracers is a promising tool to study central neuroinflammation.

Currently, a few P2X7 receptor PET tracers have been reported [46, 51–55]. We previously demonstrated that [^{18}F]JNJ-64413739 is suitable to quantify central target engagement of P2X7 therapeutic compounds [56]. Here, we evaluate [^{18}F]JNJ-64413739 as a tool to measure neuroinflammation.

To achieve this goal, we used a rat model of local neuroinflammation induced by intracerebral injection of lipopolysaccharide (LPS). We selected this model because (a) priming of Toll-like receptors (TLR) by LPS is one of the hallmarks of P2X7-mediated release of pro-inflammatory cytokines [57–59] and (b) local LPS injection results in a spatially confined region of neuroinflammation, while other, less affected regions can serve as reference [60].

We studied [^{18}F]JNJ-64413739 uptake in the LPS injected, control (PBS-injected), and reference brain regions by *in vivo* PET imaging. We compared PET imaging results to the results from *ex vivo* ARG, immunohistochemistry (IHC), and gene expression (qPCR) analysis. We confirmed the specificity of binding of [^{18}F]JNJ-64413739 to P2X7 receptors by performing competition studies with the P2X7 antagonist JNJ-54175446.

Materials and Methods

Details are provided in the electronic supplementary material (ESM).

Results

Selection of LPS Dose and Time Points: Longitudinal Pilot PET Imaging Studies with [^{18}F]JNJ-64413739

Since P2X7 tracers have not been evaluated in a rat LPS local neuroinflammation model, we first conducted a pilot imaging study with [^{18}F]JNJ-64413739 to select the optimal time points and LPS dose for subsequent imaging experiments. Details are provided in the ESM. Based on the results of this pilot experiment, 20 µg of LPS and day 2 post-LPS were selected for all subsequent experiments. Representative examples of PET images of rats injected with 0 µg of LPS (PBS control) and 20 µg of LPS, respectively, at day 1, 2, 3, and 4 post-injections are shown in Fig. 1.

Verification of Induced Neuroinflammatory Markers at Day 2 Post-LPS (20 µg): a qPCR Study

To confirm neuroinflammation induced by LPS in brain tissue, we used quantitative RT-PCR to measure messenger RNA (mRNA) levels of neuroinflammatory marker genes Tspo, Aif1, and P2rx7 in both LPS- and PBS-injected brains. The results of this experiment are summarized in Fig. 2. Expression levels of Tspo and Aif1 were more than 7 and 5 times higher in LPS-injected hemisphere than that in PBS-injected hemisphere, respectively; both genes had statistically significant main effects of treatment and hemisphere, and interaction effect involving both factors (Tspo gene, p (interaction) = 0.0019; p (LPS *vs.* PBS) = 0.0001; p (injected *vs.* contralateral) = 0.0019; Aif1 gene, p (interaction) = 0.0018; p (LPS *vs.* PBS) < 0.0001; p (injected *vs.* contralateral) = 0.0021). The mRNA level of P2rx7 was assessed, and its expression level was also found to be enhanced in the LPS-injected hemisphere compared with the PBS-injected hemisphere (significant effect of treatment, p (LPS *vs.* PBS) = 0.0002; non-significant effect of interaction or hemisphere, p = 0.18 and p = 0.40, correspondingly). The significant effect of LPS treatment found on P2X7 receptor expression indicates that this target may be a promising biomarker to detect neuroinflammation in LPS model. It should be noted that an increase of mRNA levels of all genes studied (but especially P2rx7) was detected in the contralateral hemisphere of LPS-injected compared to PBS-injected brains. This "spreading of the inflammation" may be due to the high and non-physiological level of inflammatory insult produced by local injection of relatively high dose of LPS.

Concordance Between In vivo [^{18}F]JNJ-64413739 PET Imaging, [^{18}F]JNJ-64413739 Ex vivo ARG, and Immunohistochemistry of Iba1

To study similarities between *in vivo* [^{18}F]JNJ-64413739 uptake, *ex vivo* ARG, and Iba1 IHC staining, all three assessments were performed in the same animal. First, rats were PET scanned with [^{18}F]JNJ-64413739 2 days after LPS/PBS injection. Immediately after the scan, the animals were euthanized, brains extracted, and *ex vivo* ARG was performed on 20-µm brain sections as described in the "Materials and Methods." Adjacent 10-µm sections were
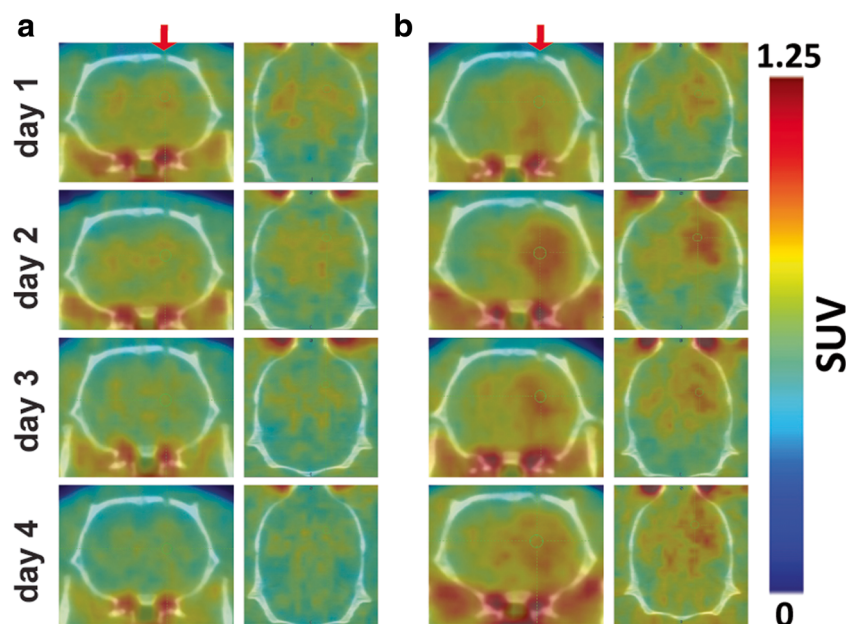
Fig. 1 Examples of *in vivo* PET imaging with [^{18}F]JNJ-64413739: PET images (summed over the entire scan period) of the rat brain (coronal view, left; horizontal view, right) injected with **a** PBS and a rat injected with **b** 20 μg of LPS. Pet images are overlaid with corresponding CT images (grayscale, – 1000 to 2500 HU). Images are centered on the injection site (the corresponding craniotomies are indicated by red arrows). Images are acquired 1–4 days post-injection.

used for the IHC staining. The *in vivo* PET scan showed markedly increased uptake (29 %, SUVs measured 20 min post-tracer injection) of [^{18}F]JNJ-64413739 at the LPS-injected site relative to the contralateral site in the LPS-injected rat (Fig. 3a), but not in the PBS-injected rat (Fig. 3e) (4 % higher uptake in the contralateral site than in the injected site, SUVs measured 20 min post-tracer injection). The *ex vivo* ARG showed a strong signal in the cortex and striatum injected with LPS (Fig. 3b), whereas a much weaker signal was detected in the corresponding site in the control (PBS-injected) animal (Fig. 3f). The difference in signals between the injected and contralateral side was 26 % in the LPS-injected rat (Fig. 3b); while in the PBS injected rat, the difference between the injected and the contralateral site constituted only 0.9 % (Fig. 3f). A similar trend was

observed in the adjacent brain sections stained for Iba1 (brain section from LPS-injected rat: Fig. 3c; brain section from PBS-injected rat: Fig. 3g; the corresponding striatal regions at the center of the injections visualized with the higher magnifications are shown in Fig. 3d and h). Because IHC and *ex vivo* ARG procedures were performed on the same tissue sections, decreased resolution of Iba1 staining in fresh frozen brain sections prevented visualization of morphology of individual microglial cells. Nevertheless, higher magnification images showed marked difference in the intensity of Iba1 staining between LPS- (Fig. 3d) and PBS (Fig. 3h)-injected rats, suggesting an increased number of microglial cells which corresponds to the increased uptake of [^{18}F]JNJ-64413739 both *in vivo* (PET scans) and *ex vivo* (ARG). Interestingly, *in vitro* ARG, in which [^{18}F]JNJ-
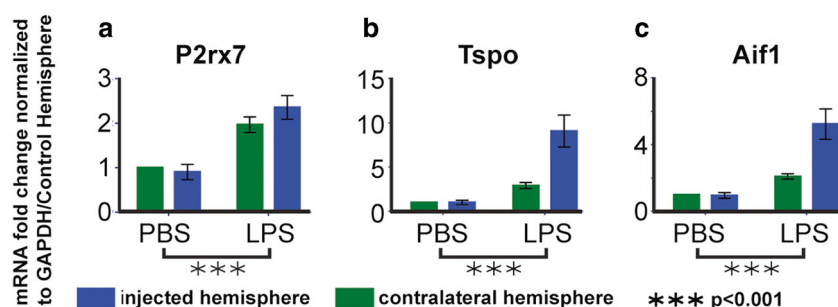

Fig. 2 Neuroinflammatory markers detected in rat brains at day 2 post-LPS (20 μg) or PBS administration: fold changes of mRNA expression of **a** P2rx7, **b** Tspo, and **c** Aif1 in LPS-injected hemisphere (± s.e.m. indicated by the error bar) compared with contralateral hemisphere in LPS-injected brains, as well as in PBS-injected brains. Data were normalized to mRNA levels of each gene from contralateral hemisphere in the PBS-injected mice. Data were analyzed by a two-way ANOVA followed by Bonferroni's post hoc test.
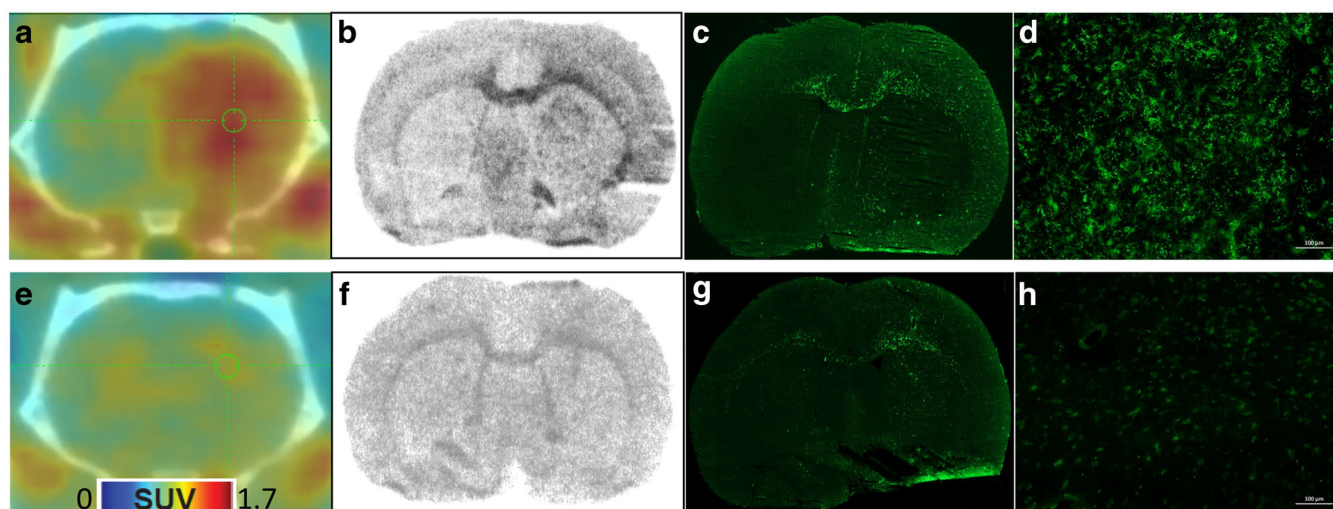
Fig. 3 Examples of *in vivo* PET/CT images with [^{18}F]JNJ-64413739 after local injection of **a** LPS and **e** PBS: coronal view centered on the center of the injection site shown by a green cursor. PET shown in color on 0 to 1.7 SUV scale, summed over the entire scan period; overlaid with corresponding CT images shown in grayscale, – 1000 to 2500 HU). *Ex vivo ARG* (**b** injected with LPS and **f** injection with PBS) and Iba1 immunostaining (low magnification, **c** and **g**; higher magnification, **d** and **h**; scale bar = 100 μm) on the same rat brain 2 days after local injection of LPS or PBS.

64413739 was directly applied to brain sections, consistently failed to detect any signal increase at the injection site (data not shown), indicating potential difference in binding *in vivo vs. in vitro*.

In vivo PET Imaging Study with [^{18}F]JNJ-64413739 in Naïve, PBS-Injected and LPS-Injected Rats

To evaluate the uptake of the [^{18}F]JNJ-64413739 by *in vivo* PET scans, we statistically compared normalized uptake (SUVR, cerebellum as a reference area) of [^{18}F]JNJ-64413739 between the injected and control sites and found significantly higher uptake of [^{18}F]JNJ-64413739 in the LPS-injected site (37 % increase in SUVRs measured over entire scan period, $n = 5$, $p = 0.0152$, t test). In contrast, there was no statistical difference between the injected and control sites in PBS-injected group (3 % increase in SUVRs in the injected site measured over entire scan period, $n = 5$, $p = 0.79$, t test) and corresponding sites in the naïve group (1.4 % difference in SUVRs measured over entire scan period, $n = 4$, $p = 0.22$, t test).

We then compared [^{18}F]JNJ-64413739 uptake at the injection site and control site across experimental groups (naïve, PBS-injected, and LPS-injected). Time-activity curves (TACs) in three VOIs (injection site, control site, and cerebellum as a reference area) in the naïve ($n = 4$), PBS-injected ($n = 5$), and LPS-injected ($n = 5$) groups are shown in Fig. 4a through c. We found no differences in [^{18}F]JNJ-64413739 uptake between injection site of the rats injected with PBS and the corresponding site in the naïve rats ($p = 0.27$, t test, SUV measured over the entire scanning

period). In contrast, injection sites of rats injected with LPS showed a significantly increased uptake of [^{18}F]JNJ-64413739 relative to those of control animals injected with PBS (34 % increase in SUV measured over entire scanning period, $p = 0.036$, t test). Uptake in contralateral hemispheres and cerebellums were not significantly different ($p = 0.80$ and $p = 0.96$, correspondingly) between these groups of animals.

Effect of JNJ-54175446 on PET Imaging with [18F]JNJ-64413739

To demonstrate specificity of increased uptake of [^{18}F]JNJ-64413739 at the LPS-injected site, we performed blocking studies with the previously reported P2X7 antagonist JNJ-54175446 [61]. The results of the displacement study are provided in the ESM.

In pre-treatment study, 10 min before starting the PET scan, JNJ-54175446 ($n = 5$) or vehicle ($n = 5$) was administered intravenously (2.25 mg/kg) to LPS-injected rats. TACs for both groups are shown in Fig. 5a and b, while Fig. 5c shows SUVR (reference: cerebellum) values (measured 30–60 min from the scan start) at each site ("LPS-injected site" and "control site") in each animal. The SUVR values are grouped by treatment condition (JNJ-54175446 or vehicle). Administration of JNJ-54175446 (2.25 mg/kg) significantly ($p < 0.05$, t test) lowered uptake (SUV) of [^{18}F]JNJ-64413739 in both injected and non-injected hemispheres relative to the corresponding hemispheres in the vehicle-control animals; however, there was a higher decrease at the injected site than at the control site (Fig.5a–c). Correspondingly, SUVR values were significantly lower ($p = 0.04$, one-
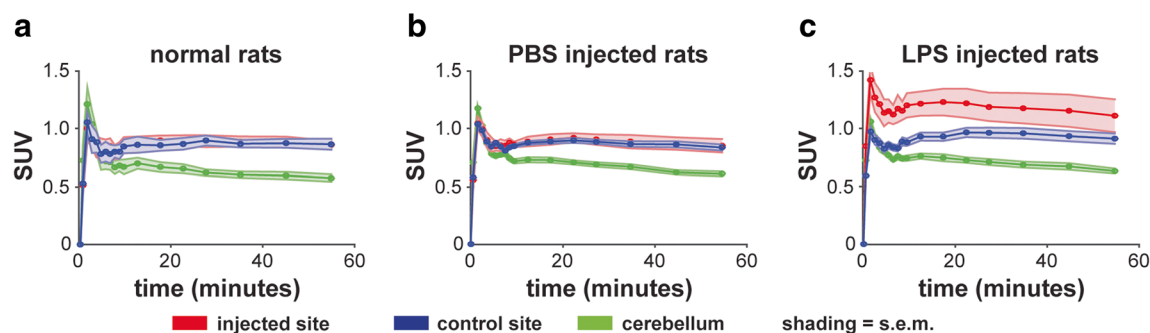
Fig. 4 The time-activity curves (TACs) of the uptake (SUV values) of [18F]JNJ-64413739 in three volumes of interest (VOIs): injected site (or corresponding VOI in the naïve group), red line; control site, blue line; and cerebellum as a reference area, green line; the shading around the lines indicates s.e.m. in three groups of rats (**a**: naïve, $n = 4$; **b**: PBS-injected, $n = 5$; **c**: LPS-injected, 20 μg, $n = 5$). The imaging session was conducted 2 days after injection (for the PBS- and LPS-injected groups).

sided t test) at the LPS-injected site in the animals treated with JNJ-54175446 than at the LPS-injected site in vehicle-dosed animals.

The results of experiments with JNJ-54175446 support the finding that the [18F]JNJ-64413739 signal at the LPS-injected site is likely specific to P2X7.

Availability of Data and Materials

The datasets used and analyzed during the current study are available from the corresponding author on reasonable request.

Discussion

We evaluated the novel P2X7 antagonist PET ligand, [18F]JNJ-64413739, in a preclinical neuroinflammatory rat model. We demonstrated increased uptake of the PET ligand at the neuroinflammatory site. These findings show promise for [18F]JNJ-64413739 as a PET ligand to study P2X7 receptors in a variety of brain disorders involving

neuroinflammation [3, 4]. We acknowledge that local LPS-induced changes in neuroinflammation, as described in our paper, are extreme and most likely do not represent neuroinflammatory changes in chronic CNS diseases; detailed discussion is provided in the ESM. Nonetheless, this model was set up to address some key scientific questions described here. We plan to extend these findings in more physiologically relevant models of chronic neuroinflammation.

In recent years, a few PET tracer candidates to image P2X7 receptors have been proposed [62], and some were evaluated in preclinical models of neuroinflammation [47, 63, 64]. For example, [11C]GSK1482160 showed increased tracer uptake in both systemic LPS (5 mg/kg) model in mice [47] and in rats with experimental autoimmune encephalomyelitis (EAE) [63]. These and other recent results [55, 56] are a promising demonstration of the potential of a P2X7 receptor tracer. However, short half-life of carbon-11 may restrict the clinical application of C-11-labeled PET tracers; it would be preferable to use F-18-labeled tracers. Prior to our work, only one F-18-labeled P2X7 receptor tracer, [18F]EFB [46], has been tested in preclinical models of
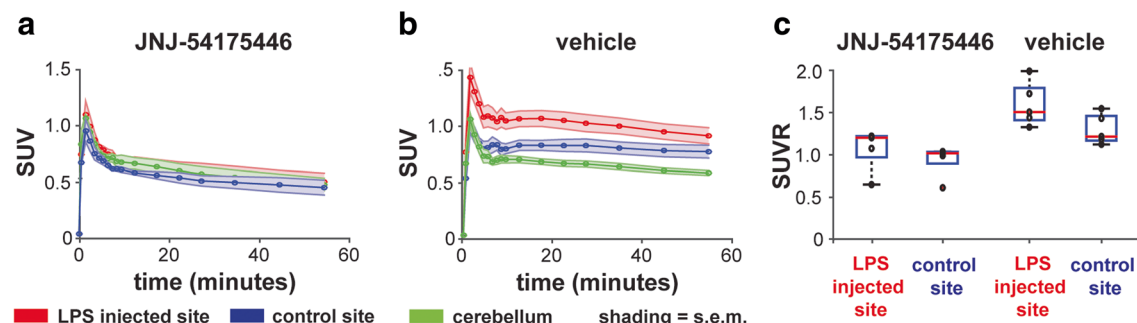

Fig. 5 TACs of SUV values of [18F]JNJ-64413739 in three VOIs (LPS-injected site, red line; control site, blue line; and cerebellum as a reference area, green line; the shading around the lines indicates s.e.m.) in two groups of LPS-injected rats ($n = 5$ in each group) plotted over time. Intravenous injection of JNJ-54175446 **a** 2.25 mg/kg, or **b** vehicle (blank formulation, 0 mg/kg, B) was administered 10 min prior to the scan. **c** SUVR (reference: cerebellum) values measured at each site ("LPS-injected site" and "control site") in each animal (indicated by "o" marker) during a period of 30–60 min after starting the scan; the SUVR values are grouped by treatment condition (JNJ-54175446 or vehicle).

neuroinflammation. The preliminary evaluation of [^{18}F] EFB was promising; however, limited brain penetration and suboptimal imaging quality may limit the use of this tracer.

We conducted PET scans with [^{18}F]JNJ-64413739 in naïve animals and animals injected either with PBS or LPS (20 μg, 2 days post-LPS). The TACs in cerebellum and contralateral site were the same in all groups of animals (Fig. 4, blue and green colors). PBS-injected sites were indistinguishable from uptake in naïve animals, indicating that the surgery did not lead to increased [^{18}F]JNJ-64413739 uptake. In contrast, we found a statistically significant increase of [^{18}F]JNJ-64413739 uptake in the LPS-injected site relative to the control site (37 % increase in SUVRs measured over entire scan period, $n = 5$, $p = 0.0152$, t test). To further confirm target specificity, we showed a significant blocking effect by using P2X7 antagonist JNJ-54175446 [61]. These findings support our proposal that the observed increase of [^{18}F]JNJ-64413739 signal at the LPS-injected site is likely specific to P2X7 receptors. The increased uptake of [^{18}F]JNJ-64413739 is most likely a consequence of LPS-induced activation of microglial cells that express P2X7 receptors, as supported by increased staining with Iba1.

To relate increased uptake of [^{18}F]JNJ-64413739 to neuroinflammation induced by LPS in brain tissue, we measured mRNA levels of neuroinflammatory marker genes Tspo, Aif1, and P2rx7 in both LPS- and PBS-injected brains. As expected, expression levels of all genes were elevated in LPS-injected hemisphere relative to PBS-injected hemisphere (more than 7, 5, 2 times for Tspo, Aif1, and P2rx7, respectively, Fig. 2). Interestingly, we also detected increased mRNA levels of all genes studied, but especially P2rx7, in the contralateral hemisphere of LPS-injected brains. This "spreading of the inflammation" represents a novel observation, at least, for the genes studied. Further studies are needed to determine whether this effect is specific to LPS or is a general neuroinflammatory phenomenon [65].

To investigate whether increased [^{18}F]JNJ-64413739 uptake corresponds to an increased number of microglial cells post-LPS administration, we compared [^{18}F]JNJ-64413739 uptake and intensity of IHC staining for the microglial marker Iba1. We performed *in vivo* PET scans, *ex vivo* ARG, and IHC staining in the same animal and used adjacent brain sections for *ex vivo* ARG and IHC staining. We found a similar increase in signals at the LPS-injected site relative to the contralateral site: PET scans, ARG, and IHC showed a 29 %, 26 %, and 25 % increase, respectively (Fig. 3, top row). The difference between injected and contralateral site in PBS-injected control rats was smaller: PET scans, ARG, and IHC showed a 4 %, 1 %, and 12 % increase, respectively (Fig. 3, bottom row). Overall, the *in vivo* PET imaging, *ex vivo* ARG and Iba1 IHC staining showed concordant results (Fig. 3).

Conclusion

The work presented in this paper demonstrates that (1) the brain regions of rats injected with LPS had a significantly increased uptake of [^{18}F]JNJ-64413739 relative to the PBS-injected controls; (2) the specificity of increased uptake at LPS-injected sites was confirmed by pre-treatment and displacement studies with specific P2X7 antagonist JNJ-54175446; and (3) the observed by *in vivo* PET increase in uptake of [^{18}F]JNJ-64413739 at the LPS-injected site was concordant with *ex vivo* autoradiography (ARG), upregulation of neuroinflammatory biomarkers, and elevated P2X7 expression levels. While further work is needed to study [^{18}F]JNJ-64413739 in other models of neuroinflammation, the current results favorably characterize [^{18}F]JNJ-64413739 as a potential imaging biomarker of central neuroinflammation and is an important step toward developing PET tracer to image neuroinflammation in the clinic.

Compliance with Ethical Standards

Ethics Approval and Consent to Participate

Consent for Publication

Not applicable

Competing Interests

The authors declare that they have no conflict of interests

Publisher's note Springer Nature remains neutral with regard to jurisdictional claims in published maps and institutional affiliations.

References

1. De Picker LJ, Morrens M, Chance SA, Boche D (2017) Microglia and brain plasticity in acute psychosis and schizophrenia illness course: a meta-review. Front Psych 8:238
2. Schain M, Kreisl WC (2017) Neuroinflammation in neurodegenerative disorders—a review. Curr Neurol Neurosci Rep 17(25)
3. Skaper SD, Facci L, Zusso M, Giusti P (2018) An inflammation-centric view of neurological disease: beyond the neuron. Front Cell Neurosci 12(72)
4. Banjara M, Ghosh C (2017) Sterile neuroinflammation and strategies for therapeutic intervention. Int J Inflam 2017:8385961
5. Knezevic D, Mizrahi R (2018) Molecular imaging of neuroinflammation in Alzheimer's disease and mild cognitive impairment. Prog Neuropsychopharmacol Biol Psych 80:123–131
6. Göbel K, Ruck T, Meuth SG (2018) Cytokine signaling in multiple sclerosis: lost in translation. Mult Scler J 24:432–439

7. Bauer ME, Teixeira AL (2018) Inflammation in psychiatric disorders: what comes first? Ann N Y Acad Sci 2018; 1–11

8. Scolding N (2014) Recognising and diagnosing inflammatory brain disease. J Neurol Neurosurg Psychiatry 85:e3

9. Janssen B, Vugts JD, Windhorst DA, Mach HR (2018) PET imaging of microglial activation—beyond targeting TSPO. Molecules 23:607

10. Holmes SE, Hinz R, Conen S, Gregory CJ, Matthews JC, Anton-Rodriguez JM, Gerhard A, Talbot PS (2018) Elevated translocator protein in anterior cingulate in major depression and a role for inflammation in suicidal thinking: a positron emission tomography study. Biol Psychiatry 83:61–69

11. Hortala L, Arnaud J, Roux P et al (2014) Synthesis and preliminary evaluation of a new fluorine-18 labelled triazine derivative for PET imaging of cannabinoid CB2 receptor. Bioorganic Med Chem Lett 24:283–287

12. Horti AG, Gao Y, Ravert HT et al (2010) Synthesis and biodistribution of [(11)C]A-836339, a new potential radioligand for PET imaging of cannabinoid type 2 receptors (CB(2)). Bioorganic Med Chem 18:5202–5207

13. Moldovan R-P, Teodoro R, Gao Y, Deuther-Conrad W, Kranz M, Wang Y, Kuwabara H, Nakano M, Valentine H, Fischer S, Pomper MG, Wong DF, Dannals RF, Brust P, Horti AG (2016) Development of a high-affinity PET radioligand for imaging cannabinoid subtype 2 receptor. J Med Chem 59:7840–7855

14. Slavik R, Herde AM, Bieri D, Weber M, Schibli R, Krämer SD, Ametamey SM, Mu L (2015) Synthesis, radiolabeling and evaluation of novel 4-oxo-quinoline derivatives as PET tracers for imaging cannabinoid type 2 receptor. Eur J Med Chem 92:554–564

15. Zhang J (2015) Mapping neuroinflammation in frontotemporal dementia with molecular PET imaging. J Neuroinflammation 12:108

16. de Vries EFJ, Doorduin J, Dierckx RA, van Waarde A (2008) Evaluation of [11C]rofecoxib as PET tracer for cyclooxygenase 2 overexpression in rat models of inflammation. Nucl Med Biol 35:35–42

17. Cao Q, Cai W, Li Z-B, Chen K, He L, Li HC, Hui M, Chen X (2007) PET imaging of acute and chronic inflammation in living mice. Eur J Nucl Med Mol Imaging 34:1832–1842

18. Wang L, Cheng R, Fujinaga M, Yang J, Zhang Y, Hatori A, Kumata K, Yang J, Vasdev N, du Y, Ran C, Zhang MR, Liang SH (2017) A facile radiolabeling of [18F]FDPA via spirocyclic iodonium ylides: preliminary PET imaging studies in preclinical models of neuroinflammation. J Med Chem 60:5222–5227

19. Airas L, Nylund M, Rissanen E (2018) Evaluation of microglial activation in multiple sclerosis patients using positron emission tomography. Front Neurol 9:181

20. Cerami C, Iaccarino L, Perani D (2017) Molecular imaging of neuroinflammation in neurodegenerative dementias: the role of in vivo PET imaging. Int J Mol Sci 18:993

21. Bloomfield PS, Selvaraj S, Veronese M, Rizzo G, Bertoldo A, Owen DR, Bloomfield MAP, Bonoldi I, Kalk N, Turkheimer F, McGuire P, de Paola V, Howes OD (2016) Microglial activity in people at ultra high risk of psychosis and in schizophrenia; an [11C]PBR28 PET brain imaging study. Am J Psychiat 173:44–52

22. Suridjan I, Pollock BG, Verhoeff NPLG, Voineskos AN, Chow T, Rusjan PM, Lobaugh NJ, Houle S, Mulsant BH, Mizrahi R (2015) In-vivo imaging of grey and white matter neuroinflammation in Alzheimer's disease: a positron emission tomography study with a novel radioligand, [18F]-FEPPA. Mol Psychiatry 20:1579–1587

23. Yokokura M, Terada T, Bunai T, Nakaizumi K, Takebayashi K, Iwata Y, Yoshikawa E, Futatsubashi M, Suzuki K, Mori N, Ouchi Y (2017) Depiction of microglial activation in aging and dementia: positron emission tomography with [11C]DPA713 versus [11C](R)PK11195. J Cereb Blood Flow Metab 37:877–889

24. Selvaraj S, Bloomfield PS, Cao B, Veronese M, Turkheimer F, Howes OD (2018) Brain TSPO imaging and gray matter volume in schizophrenia patients and in people at ultra high risk of psychosis: an [11C]PBR28 study. Schizophr Res 195:206–214

25. Di Biase MA, Zalesky A, O'Keefe G et al (2017) PET imaging of putative microglial activation in individuals at ultra-high risk for psychosis, recently diagnosed and chronically ill with schizophrenia. Transl Psychiatry 7:e1225

26. Hafizi S, Da Silva T, Gerritsen C et al (2017) Imaging microglial activation in individuals at clinical high risk for psychosis: an in vivo PET study with [18F]FEPPA. Neuropsychopharmacol 42:2474–2481

27. Narendran R, Frankle WG (2016) Comment on analyses and conclusions of "microglial activity in people at ultra high risk of psychosis and in schizophrenia: an [11C]PBR28 PET brain imaging study". Am J Psychiatry 173:536–537

28. Notter T, Coughlin JM, Gschwind T et al (2017) Translational evaluation of translocator protein as a marker of neuroinflammation in schizophrenia. Mol Psychiatry 23:323

29. Notter T, Coughlin JM, Sawa A, Meyer U (2017) Reconceptualization of translocator protein as a biomarker of neuroinflammation in psychiatry. Mol Psychiatry 23:36

30. van der Doef TF, de Witte LD, ALm S et al (2016) In vivo (R)-[11C]PK11195 PET imaging of 18kDa translocator protein in recent onset psychosis. NPJ Schizophr 2:16031

31. Ghadery C, Koshimori Y, Coakeley S, Harris M, Rusjan P, Kim J, Houle S, Strafella AP (2017) Microglial activation in Parkinson's disease using [18F]-FEPPA. J Neuroinflammation 14:8

32. Koshimori Y, Ko J-H, Mizrahi R, Rusjan P, Mabrouk R, Jacobs MF, Christopher L, Hamani C, Lang AE, Wilson AA, Houle S, Strafella AP (2015) Imaging striatal microglial activation in patients with Parkinson's disease. PLoS One 10:e0138721

33. Vivash L, O'Brien TJ (2016) Imaging microglial activation with TSPO PET: lighting up neurologic diseases? J Nucl Med 57:165–168

34. Kreisl WC, Henter ID, Innis RB (2018) Imaging translocator protein as a biomarker of neuroinflammation in dementia. In: Advances in pharmacology. Ed. Pasternak GW, Coyle JT. Academic Press, pp. 163–85

35. Ottoy J, De Picker L, Verhaeghe J et al (2018) [18F]PBR111 PET imaging in healthy controls and schizophrenia: test – retest reproducibility and quantification of neuroinflammation. J Nucl Med 59:1267–1274

36. Feeney C, Scott G, Raffel J, Roberts S, Coello C, Jolly A, Searle G, Goldstone AP, Brooks DJ, Nicholas RS, Trigg W, Gunn RN, Sharp DJ (2016) Kinetic analysis of the translocator protein positron emission tomography ligand [18F]GE-180 in the human brain. Eur J Nucl Med Mol Imaging 43:2201–2210

37. Ikawa M, Lohith TG, Shrestha S, Telu S, Zoghbi SS, Castellano S, Taliani S, da Settimo F, Fujita M, Pike VW, Innis RB (2017) 11C-ER176, a radioligand for 18-kDa translocator protein, has adequate sensitivity to robustly image all three affinity genotypes in human brain. J Nucl Med 58:320–325

38. Lagarde J, Sarazin M, Bottlaender M (2018) In vivo PET imaging of neuroinflammation in Alzheimer's disease. J Neural Transm 125:847–867

39. Tronel C, Largeau B, Santiago Ribeiro MJ, Guilloteau D, Dupont AC, Arlicot N (2017) Molecular targets for PET imaging of activated microglia: the current situation and future expectations. Int J Mol Sci 18:802

40. Gatliff J, East DA, Singh A, Alvarez MS, Frison M, Matic I, Ferraina C, Sampson N, Turkheimer F, Campanella M (2017) A role for TSPO in mitochondrial Ca(2+) homeostasis and redox stress signaling. Cell Death Dis 8:e2896

41. Guilarte TR, Loth MK, Guariglia SR (2016) TSPO finds NOX2 in microglia for redox homeostasis. Trends Pharmacol Sci 37:334–343

42. Li F, Liu J, Liu N, Kuhn LA, Garavito RM, Ferguson-Miller S (2016) Translocator protein 18 kDa (TSPO): an old protein with new functions? Biochemistry 55:2821–2831

43. Papadopoulos V, Fan J, Zirkin B (2017) Translocator protein (18 kDa): an update on its function in steroidogenesis. J Neuroendocrinol 30:e12500

44. Yasin N, Veenman L, Singh S, Azrad M, Bode J, Vainshtein A, Caballero B, Marek I, Gavish M (2017) Classical and novel TSPO ligands for the mitochondrial TSPO can modulate nuclear gene expression: implications for mitochondrial retrograde signaling. Int J Mol Sci 18:786

45. Monif M, Reid CA, Powell KL, Smart ML, Williams DA (2009) The P2X7 receptor drives microglial activation and proliferation: a trophic role for P2X7R pore. J Neurosci 29:3781–3791

46. Fantoni ER, Dal Ben D, Falzoni S, di Virgilio F, Lovestone S, Gee A (2017) Design, synthesis and evaluation in an LPS rodent model of neuroinflammation of a novel 18F-labelled PET tracer targeting P2X7. EJNMMI Res 7:31

47. Territo PR, Meyer JA, Peters JS, Riley AA, McCarthy BP, Gao M, Wang M, Green MA, Zheng QH, Hutchins GD (2017) Characterization of (11)C-GSK1482160 for targeting the P2X7 receptor as a biomarker for neuroinflammation. J Nucl Med 58:458–465

48. He Y, Taylor N, Fourgeaud L, Bhattacharya A (2017) The role of microglial P2X7: modulation of cell death and cytokine release. J Neuroinflammation 14:135

49. Bhattacharya A, Wang Q, Ao H, Shoblock JR, Lord B, Aluisio L, Fraser I, Nepomuceno D, Neff RA, Welty N, Lovenberg TW, Bonaventure P, Wickenden AD, Letavic MA (2013) Pharmacological characterization of a novel centrally permeable P2X7 receptor antagonist: JNJ-47965567. Br J Pharmacol 170:624–640

50. Lord B, Aluisio L, Shoblock JR, Neff RA, Varlinskaya EI, Ceusters M, Lovenberg TW, Carruthers N, Bonaventure P, Letavic MA, Deak T, Drinkenburg W, Bhattacharya A (2014) Pharmacology of a novel central nervous system–penetrant P2X7 antagonist JNJ-42253432. J Pharmacol Exp Ther 351:628–641

51. Ory D, Celen S, Gijsbers R, van den Haute C, Postnov A, Koole M, Vandeputte C, Andres JI, Alcazar J, de Angelis M, Langlois X, Bhattacharya A, Schmidt M, Letavic MA, Vanduffel W, van Laere K, Verbruggen A, Debyser Z, Bormans G (2016) Preclinical evaluation of a P2X7 receptor-selective radiotracer: PET studies in a rat model with local overexpression of the human P2X7 receptor and in nonhuman primates. J Nucl Med 57:1436–1441

52. Gao M, Wang M, Green MA, Hutchins GD, Zheng QH (2015) Synthesis of [^{11}C]GSK1482160 as a new PET agent for targeting P2X(7) receptor. Bioorg Med Chem Lett 25:1965–1970

53. Janssen B, Vugts Danielle J, Funke U et al (2014) Synthesis and initial preclinical evaluation of the P2X7 receptor antagonist [11C]A-740003 as a novel tracer of neuroinflammation. J Label Compd Radiopharm 57:509–516

54. Gao M, Wang M, Glick-Wilson BE, Meyer JA, Peters JS, Territo PR, Green MA, Hutchins GD, Zarrinmayeh H, Zheng QH (2018) Synthesis and preliminary biological evaluation of a novel P2X7R radioligand [18F]IUR-1601. Bioorganic Med Chem Lett 28:1603–1609

55. Janssen B, Vugts DJ, Wilkinson SM, Ory D, Chalon S, Hoozemans JJM, Schuit RC, Beaino W, Kooijman EJM, van den Hoek J, Chishty M, Doméné A, van der Perren A, Villa A, Maggi A, Molenaar GT, Funke U, Shevchenko RV, Baekelandt V, Bormans G, Lammertsma AA, Kassiou M, Windhorst AD (2018) Identification of the allosteric P2X7 receptor antagonist [^{11}C]SMW139 as a PET tracer of microglial activation. Sci Rep 8:6580

56. Koole M, Schmidt M, Hijzen A et al (2018) ^{18}F-JNJ-64413739, a novel PET ligand for the P2X7 ion channel: radiation dosimetry, kinetic modeling, test-retest variability and occupancy of the P2X7 antagonist JNJ-54175446. J Nucl Med 118:216747

57. Facci L, Barbierato M, Marinelli C et al (2014) Toll-like receptors 2, -3 and -4 prime microglia but not astrocytes across central nervous system regions for ATP-dependent interleukin-1β release. Sci Rep 4:6824

58. Spildrejorde M, Curtis SJ, Curtis BL, Sluyter R (2014) Extracellular adenosine 5′-triphosphate and lipopolysaccharide induce interleukin-1beta release in canine blood. Vet Immunol Immunopathol 157:105–110

59. Wynick C, Petes C, Tigert A, Gee K (2016) Lipopolysaccharide-mediated induction of concurrent IL-1β and IL-23 expression in THP-1 cells exhibits differential requirements for caspase-1 and cathepsin B activity. J Interf Cytokine Res 36:477–487

60. Ory D, Postnov A, Koole M, Celen S, de Laat B, Verbruggen A, van Laere K, Bormans G, Casteels C (2016) Quantification of TSPO overexpression in a rat model of local neuroinflammation induced by intracerebral injection of LPS by the use of [^{18}F]DPA-714 PET. Eur J Nucl Med Mol Imaging 43:163–172

61. Letavic MA, Savall BM, Allison BD, Aluisio L, Andres JI, de Angelis M, Ao H, Beauchamp DA, Bonaventure P, Bryant S, Carruthers NI, Ceusters M, Coe KJ, Dvorak CA, Fraser IC, Gelin CF, Koudriakova T, Liang J, Lord B, Lovenberg TW, Otieno MA, Schoetens F, Swanson DM, Wang Q, Wickenden AD, Bhattacharya A (2017) 4-Methyl-6,7-dihydro-4H-triazolo[4,5-c]pyridine-based P2X7 receptor antagonists: optimization of pharmacokinetic properties leading to the identification of a clinical candidate. J Med Chem 60:4559–4572

62. Bhattacharya A (2018) Recent advances in CNS P2X7 physiology and pharmacology: focus on neuropsychiatric disorders. Front Pharmacol 9:30

63. Han J, Liu H, Liu C, Jin H, Perlmutter JS, Egan TM, Tu Z (2017) Pharmacologic characterizations of a P2X7R-specific radioligand, [(11)C]GSK1482160 for neuroinflammatory response. Nucl Med Commun 38:372–382

64. Beaino W, Janssen B, Kooij G, van der Pol SMA, van het Hof B, van Horssen J, Windhorst AD, de Vries HE (2017) Purinergic receptors P2Y12R and P2X7R: potential targets for PET imaging of microglia phenotypes in multiple sclerosis. J Neuroinflamm 14:259

65. Hansson E (2006) Could chronic pain and spread of pain sensation be induced and maintained by glial activation? Acta Physiol 187:321–327